HTML ABSTRACT + LINKS

Highly linear and efficient phase modulators based on GaInAsP-InP three-step quantum wells

H. Mohseni[a)]
Department of Electrical and Computer Engineering, Northwestern University, Evanston, IL 60208

H. An, Z. A. Shellenbarger, M. H. Kwakernaak, and J. H. Abeles
Sarnoff Corporation, Princeton, New Jersey 08543-5300

(Received 30 September 2004; accepted 23 November 2004; published online 10 January 2005)

Highly linear and efficient phase modulators based on three-step quantum wells are reported. The spatial separation of electron and hole wave functions in the three-step quantum well leads to enhancement of the linear electro-optic component. In parallel, the quadratic electro-optic component is suppressed using a method based on tailored doping profile. Measured modulation efficiency is 48°/mm V, and the ratio of linear to quadratic components of the phase modulation is 640 at $\lambda = 1560$ nm. The efficiency is similar to the best reported values for semiconductor modulators at this wavelength, while the linearity is more than one order of magnitude higher. © *2005 American Institute of Physics*. [DOI: 10.1063/1.1854219]

Highly linear optical phase modulators are attractive for many applications including photonic analog to digital converters, laser gyroscopes, multiwavelength laser sources, beam steering, and photonic arbitrary wave form generators.[1–4] Although commonly used phase modulators based on lithium niobate have an inherent high linearity, they are not suitable for integration and have a low efficiency. In contrast, semiconductor based phase modulators are efficient and can provide a high degree of integration, but are inherently nonlinear. The main source of nonlinearity in the semiconductor phase modulators is the quadratic electro-optic (QEO) effect. Although modulators based on bulk semiconductors have smaller QEO compared with modulators based on quantum well active layers, they have significantly lower modulation efficiency. Here, we present linearized phase modulators based on GaInAsP/InP quantum wells. Measured modulator linearity is more than one order of magnitude higher than bulk GaAs and GaInAsP, while modulation efficiency is more than three times better than the bulk semiconductors. The efficiency is comparable to the best conventional quantum well modulators and more than one order of magnitude better than lithium niobate based modulators.

The active layer of our modulators is based on GaInAsP stepped quantum wells. Our earlier experiments indicate that three-step quantum wells (3SQWs) have nearly three times larger electro-optic effect compared to conventional rectangular quantum wells (RQWs).[5] A marked difference between stepped and rectangular quantum wells is the asymmetry of the stepped quantum wells that leads to spatial separation of electron and hole wave functions, resulting in an induced internal electric field.[6] Similar to the earlier report on strained AlGaN/GaN quantum wells,[7] we show that the internal electric field for a properly designed 3SQW can enhance the linear electro-optic (LEO) effect. In parallel, we reduce the quadratic electro-optic component using a method based on the adjustment of the doping profile. The combined effect of higher LEO and suppression of QEO leads to nearly 64 times improvement in linearity.

The absorption spectrum of the stepped quantum wells is modeled using an effective mass approach, and the excitonic effect is modeled with a variational method. The change of index is then calculated from the Kramers–Kronig relationship. Thickness and composition of the quantum well layers are optimized for high linearity, while keeping the absorption coefficient below $\sim 1\ \mathrm{cm}^{-1}$. The electric field inside the active region is calculated using diffusion-drift and Poisson equations.

Modulator structures are grown by low-pressure metal-organic vapor phase epitaxy on *n*-type InP substrates. Figure 1 shows the band structure of the three-stepped quantum well (3SQW) under an external electric field of 60 kV/cm. The barrier layers are InP and the composition and thickness of the layers in the quantum well from left to right are $In_{0.54}Ga_{0.46}As$ (35 Å), $In_{0.59}Ga_{0.41}As_{0.89}P_{0.11}$ (30 Å), and $In_{0.70}Ga_{0.30}As_{0.64}P_{0.36}$ (35 Å). First and second electronic wave functions ψ_{e1} and ψ_{e2}, as well as first heavy and light-hole wave functions ψ_{hh1} and ψ_{lh1} are overlapped with the band structures. Conventional phase modulators with RQW active layers are grown as references. The barrier of the rectangular quantum well is InP and the well is $In_{0.56}Ga_{0.44}As_{0.95}P_{0.05}$ (80 Å). The well width and composi-

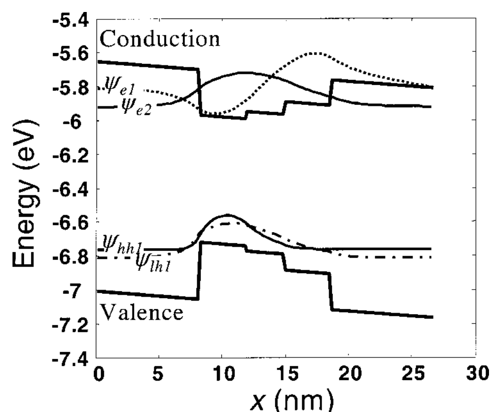

FIG. 1. Energy band structure of a 3SQW at an external electric field of 60 kV/cm. Calculated first and second electron wave functions as well as the heavy and light-hole wave functions are shown.

[a)]Electronic mail: hmohseni@ece.northwestern.edu

 © 2005 American Institute of Physics
Downloaded 26 Aug 2005 to 129.105.5.195. Redistribution subject to AIP license or copyright, see http://apl.aip.org/apl/copyright.jsp

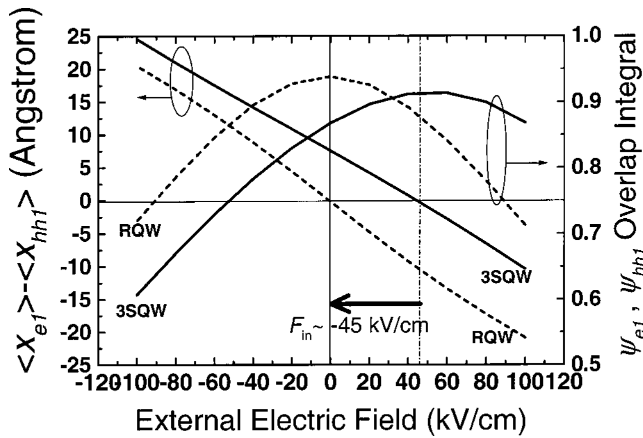

FIG. 2. Difference in average position of electron and hole in their lowest state (left axis), and their wave function overlap integral (right axis) for 3SQW and RQW structures.

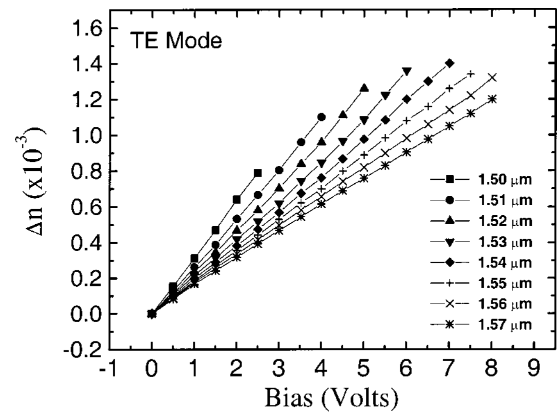

FIG. 3. Measured change of index vs the applied reverse bias at different wavelengths for a linearized phase modulator.

tion are chosen such that the energy gap of the RQW is very similar to the energy gap of the optimized 3SQW for the applied external field. The left axis of Fig. 2 compares the calculated difference between average position of the electron in its lowest state $\langle x_{e1}\rangle = \int \psi_{e1}(x) x \psi_{e1}^{*}(x)\mathrm{d}x$ and the average position of the heavy-hole in its lowest state $\langle x_{\mathrm{hh}1}\rangle = \int \psi_{\mathrm{hh}1}(x) x \psi_{\mathrm{hh}1}^{*}(x)\mathrm{d}x$ for the 3SQW and the RQW. The asymmetry of the 3SQW leads to a spatial separation of electrons and heavy-holes by more than 7 Å at zero external electric field. The displacement of the electron and heavy-hole wave functions vanishes at an external electric field of nearly 45 kV/cm. The maximum overlap between ψ_{e1} and $\psi_{\mathrm{hh}1}$ also reaches its maximum at a similar field for the 3SQW (right axis of Fig. 2). One can consider this value as an approximation for the internal electric field that is induced by the electron-hole displacement.[8] The change of index versus applied electric field can be modeled as $\Delta n(F) = -(1/2)n_0^3(r_{63}F + s_{13}F^2)$, where n_0 is the zero-field index and r_{63} and s_{13} are the linear and quadratic electro-optic coefficient.[9] In the presence of a zero-bias electric field of F_0, the change of index for a given external field F_{ex} is

$$\begin{aligned}\Delta n(F_{\mathrm{ex}}) &= \Delta n(F_{\mathrm{ex}} + F_0) - \Delta n(F_0)\\ &= -(1/2)n_0^3\{(r_{63} + 2s_{13}F_0)F_{\mathrm{ex}} + s_{13}F_{\mathrm{ex}}^2\}. \qquad (1)\end{aligned}$$

Therefore, the linear electro-optic coefficient is enhanced to $r_{63}^{*} = r_{63} + 2s_{13}F_0$. The zero-bias electric field for a conventional modulator, with a *p-i-n* structure and RQW active layer, is the built-in field in the undoped region. However, for a modulator with 3SQW active region, the zero-bias field is equal to the built-in field plus the electron-hole displacement field. Assuming an undoped region of 0.4 μm thick and *n*- and *p*-doping levels of near 10^{18} cm^{-3} in a *p-i-n* device, the built-in electric field is about -20 kV/cm. Similar to the values reported earlier,[9] we measure $r_{63} = 5.1\times10^{-10}$ cm/V and $s_{13} = -3.3\times10^{-14}$ cm^2/V^2 at $\lambda\sim1550$ nm for TE polarization. The calculated linear electro-optic coefficient is then $r_{63}^{*} = 1.83\times10^{-9}$ cm/V for the RQW, and assuming that the r_{63} and s_{13} coefficients are the same for the 3SQW, $r_{63}^{*} = 4.8\times10^{-9}$ cm/V for the 3SQW. This shows about 2.6 times higher linear electro-optic coefficient for the 3SQW compared with the RQW, which is close to the measured enhancement value of 2.8 reported earlier.[5]

Although enhancement of the linear electro-optic effect in the 3SQW is significant, the quadratic component is nearly unchanged, and hence a perfect linearization is not possible. We used the nonlinear relation between the electric field and the applied voltage to a *p-i-n* structure in order to compensate for the nonlinear relation between the change of index and the electric field. Using the depletion approximation, the external electric field F_{ex} inside the undoped region of a symmetric *p-i-n* structure is related to the external bias voltage as

$$V_{\mathrm{bias}} = -w_0F_{\mathrm{ex}} + \left(\frac{\varepsilon_s}{qN}\right)F_{\mathrm{ex}}^2, \qquad (2)$$

where w_0 is the thickness of the undoped region, N is the doping level in the *n*- and *p*-doped layers, and ε_s is the permittivity of the semiconductor. A phase modulator is perfectly linear if the change of index Δn is proportional to the applied voltage V_{bias}. Using Eqs. (1) and (2), the condition for the linearity can be calculated as

$$\frac{r_{63}^{*}}{s_{13}} = \frac{-qw_0N}{\varepsilon_s}. \qquad (3)$$

We use a 0.4-μm-thick undoped region, since it provides a single-vertical mode operation, as well as low capacitance per unit area required by high-speed traveling-wave modulators. The optimum doping level based on the depletion approximation can be calculated from Eq. (3) as $N\sim2.6\times10^{16}$ cm^{-3}. Detailed numerical simulation shows an optimum doping level of $N = 2.91\times10^{16}$ cm^{-3}.

Both 3SQW and RQW material are processed into single-mode ridge waveguides for optical and electrical measurements.

Optical absorption coefficient and change of index of the modulators are measured using Fabry–Perot oscillation shifts.[10] Figure 3 shows the measured change of index versus the applied reverse bias at different wavelengths for a linearized phase modulator. In order to compare the quadratic and linear electro-optic effects, we fit a second-order polynomial $\Delta n = A_1V + A_2V^2$ to the measured data points, and use the linear-to-quadratic coefficient ratio A_1/A_2 as a measure of linearity. Figure 4 compares the change of index versus bias of a linearized 3SQW modulator to a conventional RQW modulator at $\lambda = 1560$ nm for TE polarization. Linearized modulator shows A_1/A_2 ratio of nearly 640, while the modulator with a conventional design shows A_1/A_2 ratio of nearly

Downloaded 26 Aug 2005 to 129.105.5.195. Redistribution subject to AIP license or copyright, see http://apl.aip.org/apl/copyright.jsp

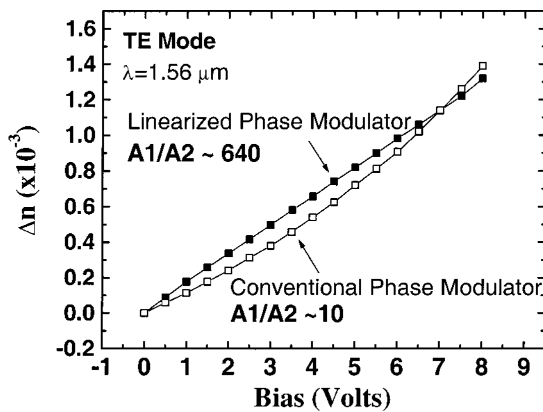

FIG. 4. Change of index vs reverse bias values for a linearized 3SQW modulator compared to a conventional RQW modulator at $\lambda = 1560$ nm for TE polarization. The linear-quadratic ration A_1/A_2 is indicated for each trace.

10. The modulation efficiency is about 48°/mm V with an optical absorption coefficient below $\sim 1\ \mathrm{cm}^{-1}$. Since the overall phase modulation consists of linear and quadratic components, suppression of the quadratic component inevitably reduces the phase efficiency. However, enhancement of the linear component in the 3SQW modulator compensates for this effect, and modulation efficiency is comparable to the efficiency of the best conventional quantum wells, and more than three times better than the efficiency of bulk semiconductors.[11–13] Also, modulator efficiency is more than one order of magnitude higher than the efficiency of modulators based on lithium niobate.[14] The linear-to-quadratic coefficient ratio is about 640, which is about 64 times better than the conventional quantum wells, and more than one order of magnitude better than bulk semiconductors.[11,12]

In conclusion, we have demonstrated linearized phase modulators based on 3SQW active layers and a modified doping profile. The enhancement of linear component of the phase modulation is believed to be the result of an internal electric field in 3SQWs, and the suppression of the quadratic component is due to the modified doping profile. The linearized devices show higher efficiency and linearity than the existing devices based on semiconductor bulk and quantum well active layers.

[1] C. Laskoskie, H. Hung, T. El-wailly, and C. Chang, J. Lightwave Technol. **7**, 600 (1989).
[2] T. Yilmaz, C. M. Christopher, M. DePriest, T. Turpin, J. H. Abeles, and P. J. Delfyett, IEEE Photonics Technol. Lett. **14**, 1608 (2002).
[3] M. Currie, T. R. Clark, and P. J. Matthews, IEEE Photonics Technol. Lett. **12**, 1689 (2000).
[4] E. Shekel, D. Majer, G. Matmon, A. Krauss, S. Ruschin, T. McDermott, M. Birk, M. Boroditsky, Lasers, and Electro-Optics Society, The 15th Annual Meeting of the IEEE, 2002, Vol. 2, p. 371.
[5] H. Mohseni, H. An, Z. A. Shellenbarger, M. H. Kwakernaak, and J. H. Abeles, Appl. Phys. Lett. **84**, 1823 (2004).
[6] S. Waywood, A. Lim, R. Gupta, S. Emery, J. Hogg, V. Heer, P. Stavrinou, M. Hopkinson, and G. Hill, J. Appl. Phys. **94**, 3222 (2003).
[7] H. Jiang and J. Singh, Appl. Phys. Lett. **75**, 1932 (1999).
[8] P. Stavrinou, S. Haywood, and G. Parry, Appl. Phys. Lett. **64**, 1251 (1993).
[9] J. Zucker, I. Bar-Joseph, B. Miller, U. Koren, and D. Chemla, Appl. Phys. Lett. **54**, 10 (1989).
[10] T. R. Walker, Electron. Lett. **21**, 581 (1985).
[11] S. Lee, R. Ramaswamy, and V. Sundaram, IEEE J. Quantum Electron. **27**, 726 (1991).
[12] A. Alping and L. Coldren, J. Appl. Phys. **61**, 2430 (1987).
[13] G. Flamand, K. De Mesel, I. Moerman, B. Dhoedt, W. Hunziker, A. Kalmar, R. Baets, P. Van Daele, and W. Leeb, IEEE Photonics Technol. Lett. **12**, 876 (2000).
[14] N. Dagli, IEEE Trans. Microwave Theory Tech. **47**, 1151 (1999).

Downloaded 26 Aug 2005 to 129.105.5.195. Redistribution subject to AIP license or copyright, see http://apl.aip.org/apl/copyright.jsp